

1 **Comment on “Climate consequences of hydrogen emissions” by Ocko and**  
2 **Hamburg (2022)**

3 **Lei Duan<sup>1,2,\*</sup> and Ken Caldeira<sup>1,3</sup>**

4 <sup>1</sup>Carnegie Institution for Science, Stanford, California, USA.

5 <sup>2</sup>Orca Sciences LLC, Kirkland, Washington, USA.

6 <sup>3</sup>Breakthrough Energy LLC, Kirkland, Washington, USA.

7 \*Correspondence to: Lei Duan ([leiduan@carnegiescience.edu](mailto:leiduan@carnegiescience.edu))

8 **Abstract**

9 In this commentary, we provide additional context for Ocko and Hamburg (2022) related to the  
10 climate consequences of replacing fossil fuels with clean hydrogen alternatives. We first provide  
11 a tutorial for the derivations of underlying differential equations that describe the radiative  
12 forcing of hydrogen emissions, which differ slightly from equations relied on by previous  
13 studies. Ocko and Hamburg (2022) defined a metric based on time-integrated radiative forcing  
14 from continuous emissions. To complement their analysis, we further present results for  
15 temperature and radiative forcing over the next centuries for unit pulse and continuous emissions  
16 scenarios. Our results are qualitatively consistent with previous studies, including Ocko and  
17 Hamburg (2022). Our results clearly show that for the same quantity of emissions, hydrogen  
18 shows a consistently smaller climate impact than methane. As with other short-lived species, the  
19 radiative forcing from a continuous emission of hydrogen is proportional to emission rates,  
20 whereas the radiative forcing from a continuous emission of carbon dioxide is closely related to  
21 cumulative emissions. After a cessation of clean hydrogen consumption, the earth cools rapidly,  
22 whereas after a cessation of carbon dioxide emissions, the earth continues to warm somewhat  
23 and remains warm for many centuries. Regardless, our results support the conclusion of Ocko  
24 and Hamburg (2022) that, if methane were a feedstock for hydrogen production, any possible  
25 near-term consequences will depend primarily on methane leakage, and secondarily on hydrogen  
26 leakage.

## 27 **1. Introduction**

28 In a recent paper, Ocko and Hamburg (2022) examined the climate consequences of replacing  
29 fossil fuel technologies with clean hydrogen alternatives. The paper accounted for a range of  
30 hydrogen and methane emission rates for two types of clean hydrogen production pathways, i.e.,  
31 green hydrogen produced via renewables and water, and blue hydrogen produced via steam  
32 methane reforming with carbon capture, usage, and storage (CCUS). They calculated the time-  
33 integrated radiative forcing using equations derived recently for hydrogen based on chemistry-  
34 climate modeling experiments (Warwick et al., 2022). Ocko and Hamburg (2022) found that  
35 high emission rates of hydrogen could diminish net climate benefits of clean hydrogen  
36 technologies, and high emissions rates of methane might lead to net climate disbenefits for blue  
37 hydrogen in the near term (e.g., 20-year timescale).

38 Here we provide context for understanding the results of Ocko and Hamburg (2022) in three  
39 different ways: (1) We present equations underlying the time evolution of hydrogen and its  
40 radiative and thermal consequences, and solve them analytically for a unit pulse and continuous  
41 hydrogen emissions scenarios; (2) We present global mean temperature and radiative forcing in  
42 the time domain; (3) We examine three emission scenarios, including a unit pulse emission, a  
43 limited-duration (square-wave) emission, and continuous emissions. Our aim here is to  
44 complement Ocko and Hamburg (2022), which emphasizes the near term, with an analysis that  
45 places greater emphasis on long-term outcomes using newly developed equations.

## 46 **2. Methods and Equations**

47 We estimate the global mean temperature change from emissions of CO<sub>2</sub>, CH<sub>4</sub>, or H<sub>2</sub> using a  
48 linearized Green's function approach, and apply these equations to simple idealized cases. We  
49 derive and apply the equations underlying the estimate of radiative forcing from hydrogen  
50 emissions as presented by Warwick et al. (2022), relying heavily on parameter values from Ocko  
51 and Hamburg (2022), Table S1. Equations describing the radiative forcing of CO<sub>2</sub> and CH<sub>4</sub> is  
52 based on Myhre et al. (2013). The calculation of the global mean temperature response is based  
53 on Gasser et al. (2017).

### 54 **2.1. Indirect forcing from hydrogen**

55 The system that describes the radiative forcing from hydrogen emissions modeled by Warwick et  
 56 al. (2022) and later used by Ocko and Hamburg (2022) is a representation of the following  
 57 underlying differential equations.

58 The change of H<sub>2</sub> molar mass relative to an unperturbed background condition, as a function of  
 59 the time horizon  $t$  in units of year, is represented by a source function  $f_{H_2}(t)$  and a decay term  
 60  $\frac{m_{H_2}}{\tau_{H_2}}$ , where  $m_{H_2}$  is the molar mass of hydrogen and  $\tau_{H_2}$  is the perturbation lifetime of H<sub>2</sub>:

$$61 \quad \frac{dm_{H_2}}{dt} = f_{H_2}(t) - \frac{m_{H_2}}{\tau_{H_2}} \quad (1)$$

62 The presence of additional hydrogen in the atmosphere changes the decay of atmospheric  
 63 methane (CH<sub>4</sub>), and also results in the production of ozone (O<sub>3</sub>) and stratospheric water vapor  
 64 (H<sub>2</sub>O). Underlying equations for perturbations to atmospheric molar masses of CH<sub>4</sub>, O<sub>3</sub>, and  
 65 stratospheric H<sub>2</sub>O induced from additional atmospheric H<sub>2</sub> (denoted by superscribe) are:

$$66 \quad \frac{dm_{CH_4}^{H_2}}{dt} = a_{CH_4} m_{H_2} - \frac{m_{CH_4}^{H_2}}{\tau_{CH_4}} \quad (2a)$$

$$67 \quad \frac{dm_{O_3}^{H_2}}{dt} = a_{O_3} m_{H_2} - \frac{m_{O_3}^{H_2}}{\tau_{O_3}} \quad (2b)$$

$$68 \quad \frac{dm_{H_2O}^{H_2}}{dt} = a_{H_2O} m_{H_2} - \frac{m_{H_2O}^{H_2}}{\tau_{H_2O}} \quad (2c)$$

69 where  $m_{CH_4}^{H_2}$ ,  $m_{O_3}^{H_2}$ , and  $m_{H_2O}^{H_2}$  are molar masses of CH<sub>4</sub>, O<sub>3</sub>, and H<sub>2</sub>O resulting from additional  
 70 atmospheric H<sub>2</sub>,  $a_{CH_4}$ ,  $a_{O_3}$ , and  $a_{H_2O}$  are factors representing the impact of remaining hydrogen  
 71 in the atmosphere on the atmospheric molar mass of different species, and  $\tau_{CH_4}$ ,  $\tau_{O_3}$ , and  $\tau_{H_2O}$   
 72 are perturbation lifetime of these species.

73 For the special case of a unit pulse perturbation of hydrogen into an unperturbed background  
 74 condition at time zero, these equations can be solved analytically. The solutions to equations (1)  
 75 and (2) under conditions  $m_{H_2}(0) = 1$ ,  $f_{H_2}(t) = 0$ ,  $m_{CH_4}^{H_2}(0) = 0$ ,  $m_{O_3}^{H_2}(0) = 0$ , and  $m_{H_2O}^{H_2}(0) =$   
 76 0 are:

$$77 \quad m_{H_2}(t) = e^{-\frac{t}{\tau_{H_2}}} \quad (3)$$

$$78 \quad m_{CH_4}^{H_2}(t) = \frac{a_{CH_4}}{\left(\frac{1}{\tau_{H_2}}\right) - \left(\frac{1}{\tau_{CH_4}}\right)} \left( e^{-\frac{t}{\tau_{CH_4}}} - e^{-\frac{t}{\tau_{H_2}}} \right) \quad (4a)$$

$$79 \quad m_{O_3}^{H_2}(t) = \frac{a_{O_3}}{\left(\frac{1}{\tau_{H_2}}\right) - \left(\frac{1}{\tau_{O_3}}\right)} \left( e^{-\frac{t}{\tau_{O_3}}} - e^{-\frac{t}{\tau_{H_2}}} \right) \quad (4b)$$

$$80 \quad m_{H_2O}^{H_2}(t) = \frac{a_{H_2O}}{\left(\frac{1}{\tau_{H_2}}\right) - \left(\frac{1}{\tau_{H_2O}}\right)} \left( e^{-\frac{t}{\tau_{H_2O}}} - e^{-\frac{t}{\tau_{H_2}}} \right) \quad (4c)$$

81 and the corresponding radiative forcing is the product of resulted molar mass and scaling factors  
 82  $A_{CH_4}$ ,  $A_{O_3}$ , and  $A_{H_2O}$  that convert molar mass to  $W m^{-2}$ . The chemically-adjusted radiative  
 83 forcing,  $A_{CH_4}^*$ , from methane forcing uses factors  $f_1$  and  $f_2$  (Myhre et al., 2013) to represent the  
 84 effect on ozone and stratospheric water vapor:

$$85 \quad A_{CH_4}^* = (1 + f_1 + f_2)A_{CH_4} \quad (5)$$

86 The indirect radiative forcing from a unit pulse emission of hydrogen,  $R_{H_2}$ , is thus the sum of  
 87 radiative forcing from all three radiatively active perturbations:

$$88 \quad R_{H_2}(t) = A_{CH_4}^* m_{CH_4}^{H_2}(t) + A_{O_3} m_{O_3}^{H_2}(t) + A_{H_2O} m_{H_2O}^{H_2}(t) \quad (6a)$$

89 Inserting equation (4) we have:

$$90 \quad R_{H_2}(t) = \frac{A_{CH_4}^* a_{CH_4}}{\left(\frac{1}{\tau_{H_2}}\right) - \left(\frac{1}{\tau_{CH_4}}\right)} \left( e^{-\frac{t}{\tau_{CH_4}}} - e^{-\frac{t}{\tau_{H_2}}} \right)$$

$$91 \quad + \frac{A_{O_3} a_{O_3}}{\left(\frac{1}{\tau_{H_2}}\right) - \left(\frac{1}{\tau_{O_3}}\right)} \left( e^{-\frac{t}{\tau_{O_3}}} - e^{-\frac{t}{\tau_{H_2}}} \right) + \frac{A_{H_2O} a_{H_2O}}{\left(\frac{1}{\tau_{H_2}}\right) - \left(\frac{1}{\tau_{H_2O}}\right)} \left( e^{-\frac{t}{\tau_{H_2O}}} - e^{-\frac{t}{\tau_{H_2}}} \right) \quad (6b)$$

92 For a 1 kg unit pulse emission case, the time-integrated radiative forcing to a specified time  
 93 horizon,  $H$ , is defined to be the Absolute Global Warming Potential (AGWP) (Myhre et al.,  
 94 2013). Thus, AGWP can be represented as:

$$95 \quad AGWP_{H_2}(H) = \int_0^H R_{H_2}(t) dt . \quad (7a)$$

96 which can be rewritten as:

$$\begin{aligned}
97 \quad AGWP_{H_2}(H) = & \frac{A_{CH_4}^* a_{CH_4} \tau_{H_2} \tau_{CH_4} \left( \tau_{CH_4} \left( 1 - e^{-\frac{H}{\tau_{CH_4}}} \right) - \tau_{H_2} \left( 1 - e^{-\frac{H}{\tau_{H_2}}} \right) \right)}{\tau_{CH_4} - \tau_{H_2}} \\
& + \frac{A_{O_3} a_{O_3} \tau_{H_2} \tau_{O_3} \left( \tau_{O_3} \left( 1 - e^{-\frac{H}{\tau_{O_3}}} \right) - \tau_{H_2} \left( 1 - e^{-\frac{H}{\tau_{H_2}}} \right) \right)}{\tau_{O_3} - \tau_{H_2}} \\
& + \frac{A_{H_2O} a_{H_2O} \tau_{H_2} \tau_{H_2O} \left( \tau_{H_2O} \left( 1 - e^{-\frac{H}{\tau_{H_2O}}} \right) - \tau_{H_2} \left( 1 - e^{-\frac{H}{\tau_{H_2}}} \right) \right)}{\tau_{H_2O} - \tau_{H_2}}
\end{aligned} \tag{7b}$$

98 Equation (7) is the response to a unit pulse emission of hydrogen taking into consideration  
99 radiative forcing adjustments to methane as in Ocko and Hamburg (2022). Because we are  
100 considering a linear system, we can use this impulse response function to derive the radiative  
101 forcing from an arbitrary hydrogen emission function  $f_{H_2}$ :

$$102 \quad \widehat{R}_{H_2}(t) = \int_0^t f_{H_2}(\tau) R_{H_2}(t - \tau) d\tau \tag{8}$$

103 Considering a continuous unit emission scenario where:

$$104 \quad f_{H_2}(t) = 1 \tag{9}$$

105 which leads to radiative forcing under a continuous emission scenario:

$$\begin{aligned}
106 \quad R_{H_2,cont}(t) = & \frac{A_{CH_4}^* a_{CH_4} \tau_{H_2} \tau_{CH_4} \left( \tau_{H_2} \left( e^{-\frac{t}{\tau_{H_2}}} - 1 \right) - \tau_{CH_4} \left( e^{-\frac{t}{\tau_{CH_4}}} - 1 \right) \right)}{\tau_{CH_4} - \tau_{H_2}} \\
& + \frac{A_{O_3} a_{O_3} \tau_{H_2} \tau_{O_3} \left( \tau_{H_2} \left( e^{-\frac{t}{\tau_{H_2}}} - 1 \right) - \tau_{O_3} \left( e^{-\frac{t}{\tau_{O_3}}} - 1 \right) \right)}{\tau_{O_3} - \tau_{H_2}} \\
& + \frac{A_{H_2O} a_{H_2O} \tau_{H_2} \tau_{H_2O} \left( \tau_{H_2} \left( e^{-\frac{t}{\tau_{H_2}}} - 1 \right) - \tau_{H_2O} \left( e^{-\frac{t}{\tau_{H_2O}}} - 1 \right) \right)}{\tau_{H_2O} - \tau_{H_2}}
\end{aligned} \tag{10}$$

107 In a linear system, the time-integrated radiative forcing from a unit pulse emission to some time  
108 horizon  $t_0$  is mathematically equivalent to the radiative forcing at time  $t_0$  from a sustained unit  
109 emission:

110 
$$AGWP_{H_2}(t_0) = R_{H_2,cont}(t_0) \quad (11)$$

111 Therefore, Ocko and Hamburg (2022) used a metric that is equal to the time integrated radiative  
 112 forcing of sustained emission to time horizon H. Since AGWP has been defined as the time-  
 113 integrated radiative forcing from the instantaneous release of 1 kg of a trace substance (Myhre et  
 114 al., 2013), here we define the time-integrated radiative forcing under a continuous emission  
 115 scenario as CAGWP:

116 
$$CAGWP_{H_2}(H) = \int_0^H R_{H_2,cont}(t) dt \quad (12a)$$

117 
$$= \int_0^H \int_0^t R_{H_2}(\tau) d\tau dt \quad (12b)$$

118 
$$= \int_0^H \int_t^H R_{H_2}(\tau) dt d\tau \quad (12c)$$

119 
$$= \int_0^H \left( \int_t^H dt \right) R_{H_2}(\tau) d\tau \quad (12d)$$

120 
$$= \int_0^H (H - t) R_{H_2}(t) dt \quad (12e)$$

121 Comparing Equation (12) with Equation (7a), we can see that the CAGWP metric is equivalent  
 122 to the AGWP metric, except that the radiative forcing at time 0 is weighted by H, and the  
 123 radiative forcing at time H is weighted at 0, with a linear ramping of weights in-between by the  
 124 number of years to the end of the time horizon. Equation (12) illustrates that time-integrated  
 125 metrics under sustained emissions put heavy weights on the short-term effect.

126 Expanding Equation (12), we have:

127 
$$CAGWP_{H_2}(H) = \frac{A_{CH_4}^* a_{CH_4} \tau_{H_2} \tau_{CH_4} \left( \tau_{H_2}^2 \left( 1 - e^{-\frac{H}{\tau_{H_2}}} \right) - \tau_{CH_4}^2 \left( 1 - e^{-\frac{H}{\tau_{CH_4}}} \right) + H(\tau_{CH_4} - \tau_{H_2}) \right)}{\tau_{CH_4} - \tau_{H_2}}$$

128 
$$+ \frac{A_{O_3} a_{O_3} \tau_{H_2} \tau_{O_3} \left( \tau_{H_2}^2 \left( 1 - e^{-\frac{H}{\tau_{H_2}}} \right) - \tau_{O_3}^2 \left( 1 - e^{-\frac{H}{\tau_{O_3}}} \right) + H(\tau_{O_3} - \tau_{H_2}) \right)}{\tau_{O_3} - \tau_{H_2}} \quad (13)$$

$$129 \quad + \frac{A_{H_2O} a_{H_2O} \tau_{H_2} \tau_{H_2O} \left( \tau_{H_2}^2 \left( 1 - e^{-\frac{H}{\tau_{H_2}}} \right) - \tau_{H_2O}^2 \left( 1 - e^{-\frac{H}{\tau_{H_2O}}} \right) + H(\tau_{H_2O} - \tau_{H_2}) \right)}{\tau_{H_2O} - \tau_{H_2}}$$

130 Equations (10) and (13) consider continuous emissions through the whole period. Equations  
 131 considering a continuous emission to time  $tp$  are shown in the **Supplementary Information**  
 132 **Text S1**. Reproductions of the three components in Warwick et al. (2022) and Ocko and  
 133 Hamburg (2022) are shown in **Text S2**. When used to estimate radiative forcing for identical  
 134 cases, numerical differences between our equations and equations presented by Warwick et al.  
 135 (2022) are small and are unlikely to make a material difference.

## 136 2.2. Forcing from CO<sub>2</sub> and CH<sub>4</sub>

137 Here we show radiative forcing and time-integrated radiative forcing functions for carbon  
 138 dioxide (CO<sub>2</sub>) and methane emissions (CH<sub>4</sub>). Radiative forcing for a unit pulse emission of CO<sub>2</sub>  
 139 and CH<sub>4</sub> is represented as (Myhre et al., 2013):

$$140 \quad R_{CO_2}(t) = A_{CO_2} \left( a_0 + \sum_{i=1}^3 a_i e^{-\frac{t}{\tau_i}} \right) \quad (14)$$

$$141 \quad R_{CH_4}(t) = (1 + f_1 + f_2) A_{CH_4} e^{-\frac{t}{\tau_{CH_4}}} \quad (15)$$

142 And AGWP for a unit pulse emission is:

$$143 \quad AGWP_{CO_2}(H) = A_{CO_2} \left( a_0 H + \sum_{i=1}^3 a_i \tau_i \left( 1 - e^{-\frac{H}{\tau_i}} \right) \right) \quad (16)$$

$$144 \quad AGWP_{CH_4}(H) = (1 + f_1 + f_2) A_{CH_4} \tau_{CH_4} \left( 1 - e^{-\frac{H}{\tau_{CH_4}}} \right) \quad (17)$$

145 Radiative forcing for continuous emissions of CO<sub>2</sub> and CH<sub>4</sub> can be represented as:

$$146 \quad R_{CO_2,cont}(t) = A_{CO_2} \left( a_0 t + \sum_{i=1}^3 a_i \tau_i \left( 1 - e^{-\frac{t}{\tau_i}} \right) \right) \quad (18)$$

$$147 \quad R_{CH_4,cont}(t) = (1 + f_1 + f_2) A_{CH_4} \tau_{CH_4} \left( 1 - e^{-\frac{t}{\tau_{CH_4}}} \right) \quad (19)$$

148 And corresponding CAGWP is:



149 
$$CAGWP_{CO_2}(H) = A_{CO_2} \left( \frac{a_0 H^2}{2} + \sum_{i=1}^3 a_i \tau_i \left( H + \tau_i \left( e^{-\frac{H}{\tau_i}} - 1 \right) \right) \right) \quad (20)$$

150 
$$CAGWP_{CH_4}(H) = (1 + f_1 + f_2) A_{CH_4} \tau_{CH_4} \left( H + \tau_{CH_4} \left( e^{-\frac{H}{\tau_{CH_4}}} - 1 \right) \right) \quad (21)$$

151 **2.3. The global mean temperature response**

152 For a linear system, the absolute global temperature change potential (AGTP), defined as change  
 153 of global mean surface temperature realized at a given time horizon from a pulse or continuous  
 154 emission of any gas  $i$ , can be represented as a convolution function (Myhre et al., 2013; Gasser  
 155 et al., 2017):

156 
$$AGTP_i(H) = \int_0^H R_i(t) T(H - t) dt \quad (22)$$

157 In equation (22),  $R_i(t)$  is the radiative forcing for a unit pulse or continuous emission of gas  $i$ ,  
 158 and  $T(t)$  indicates the temperature response to a unit forcing that can be represented as a sum of  
 159 exponentials:

160 
$$T(t) = \lambda \sum_{j=1}^M \frac{c_j}{d_j} e^{-\frac{t}{d_j}} \quad (23)$$

161 Where  $\lambda$  is a constant that corresponds to the equilibrium climate sensitivity,  $\sum_{j=1}^M c_j = 1$ , and  $d_j$   
 162 is the response time. Two exponential terms ( $M = 2$ ) are normally used in previous studies, with  
 163 the first term be associated with the response of the ocean mixed layer and the higher order be  
 164 associated with the response of the deep ocean (Gasser et al., 2017). In our central cases, we  
 165 focus on using the equation from (Geoffroy et al., 2013):

166 
$$T(t) = 0.885 \left( \frac{0.587}{4.1} e^{-\frac{t}{4.1}} + \frac{0.413}{249} e^{-\frac{t}{249}} \right) \quad (24)$$

167 Uncertainty in the temperature response function is shown in **Text S3**.

168 **2.4. Simulations and assumptions**

169 As in Ocko and Hamburg (2022), we focus on comparing the climate impact of replacing fossil  
 170 fuel technologies with clean hydrogen alternatives. Climate impacts from hydrogen or fossil

171 fuels are the summation of climate impacts of one or more components in a linear system (Text  
172 S4).

173 In this commentary, we analyze the climate impact per 1 kg consumptions of green and blue  
174 hydrogen, and corresponding impacts from the avoided CO<sub>2</sub> emissions. We consider consistent  
175 assumptions as in Ocko and Hamburg (2022). For example, the kg amount of methane required  
176 to produce blue hydrogen is 3 times the kg amount of hydrogen used; 1 kg consumption of  
177 hydrogen would avoid 11 kg of CO<sub>2</sub> emissions (additional cases, i.e., 5 kg or 15 kg of avoided  
178 CO<sub>2</sub> emissions, are examined as well); and burning 1 kg of natural gas or methane would emit  
179 2.75 kg of CO<sub>2</sub>. Also, we take the same emission rates for methane and hydrogen to generate two  
180 central cases: a low leakage case with a 1% hydrogen and a 1% methane leakage rate, and a high  
181 leakage case with a 10% hydrogen and a 3% methane leakage rate (see detailed discussion  
182 underlying these assumptions in their paper).

183 We focus our discussions on three emission scenarios: a 1 kg pulse consumption, a 0.01 kg yr<sup>-1</sup>  
184 continuous consumption lasting for 100 years, and a 0.01 kg yr<sup>-1</sup> continuous consumption lasting  
185 for 500 years. Results for 20-, 100-, 500-year horizons are summarized in Table S2 to S5.

## 186 **Results**

187 **Climate impact of individual gas.** We first examine the time-evolving climate impact from  
188 emissions of carbon dioxide (CO<sub>2</sub>), methane (CH<sub>4</sub>), and hydrogen (H<sub>2</sub>), respectively. Similarly,  
189 we consider three emission scenarios: a 1 kg pulse emission, a 0.01 kg yr<sup>-1</sup> continuous emission  
190 lasting for 100 years, and a 0.01 kg yr<sup>-1</sup> continuous emission lasting for 500 years.

191 Figure 1 shows the climate impact of individual species under various emission scenarios.  
192 Results showing ratios of methane and hydrogen to CO<sub>2</sub> are plotted in Figure S1. For the 1 kg  
193 pulse emission scenario, all species produce the largest climate impacts within the first few years  
194 and decay over time. Soon after emission, per kg emitted, methane and hydrogen show much  
195 larger impacts compared to CO<sub>2</sub>. The global warming potential is typically defined for a 1 kg  
196 pulse emission of gas (Myhre et al., 2013), which will lead to different immediate changes in  
197 their atmospheric concentration when viewed on a molar basis. Figure S2 shows that when  
198 considering the same 1 ppb increase of these gases, methane still generates a much larger  
199 warming potential, whereas hydrogen and CO<sub>2</sub> show the same order of magnitude impacts on  
200 radiative forcing and temperature response in the first decade.

201 The climate impact of methane and hydrogen decays substantially faster than CO<sub>2</sub> along with  
202 their concentrations (perturbation lifetime used is 11.8 years for methane and 1.9 years for  
203 hydrogen). For example, the radiative forcing of methane and hydrogen for the 1 kg pulse  
204 emission scenario is smaller than that of CO<sub>2</sub> after ~ 65 and 50 years, and approaches zero after  
205 100 years. We do not consider conversions of the decayed CH<sub>4</sub> to CO<sub>2</sub>, which will add more  
206 long-term impacts for CH<sub>4</sub> emissions (Forster et al., 2021) as shown in Fig.S3. This conversion  
207 should not be considered in the case of CH<sub>4</sub> perturbations brought about by H<sub>2</sub> emissions,  
208 because there is no net addition of carbon to the atmosphere in this case. In contrast, the radiative  
209 forcing of CO<sub>2</sub> is still 28% of its maximum value at the 500-year time horizon. Temperature  
210 response behaves similarly to radiative forcing, but at a slower rate due to the inertia of the  
211 climate system. Impacts of considering different hydrogen perturbation lifetimes (i.e., 1.4 and 2.5  
212 years) are shown in Figure S4.

213 For 0.01 kg yr<sup>-1</sup> continuous emission cases, there is an accumulation of CO<sub>2</sub> concentration in the  
214 atmosphere, leading to monotonic increases in radiative forcing and temperature rise. If  
215 emissions stop abruptly after 100 years, the climate impacts of CO<sub>2</sub> slowly converge with those  
216 under the 1 kg emission case and stay roughly stable, because effects of atmospheric  
217 concentration decrease are approximately offset by effects of ocean warming. Due to the shorter  
218 perturbation lifetime of methane and hydrogen, their atmospheric concentrations reach  
219 equilibrium under continuous emission scenarios with magnitudes depending on the emission  
220 rates, and radiative forcing reaches a stable level after a few decades. Global mean temperature  
221 continues to increase slowly due to the thermal inertia of the climate system. If emissions stop  
222 abruptly after 100 years, their concentrations would decrease rapidly, and reach zero within  
223 decades. The longer perturbation lifetime of CO<sub>2</sub> results in more prominent longer-term climate  
224 impacts under both pulse and continuous emission scenarios.

225 **Climate impact of hydrogen and fossil fuels.** We now consider climate impact from hydrogen  
226 consumptions. Under the low leakage scenario (i.e., 1% hydrogen and 1% methane leakage rate),  
227 both green and blue hydrogen produce smaller radiative forcing and global mean temperature  
228 increases compared to the avoided CO<sub>2</sub> emissions (Fig. 2 and 3), indicating net climate benefits  
229 of replacing fossil fuels with clean hydrogen alternatives. Compared to green hydrogen, leakages  
230 of methane from blue hydrogen add substantial additional warming within the first few decades.  
231 For the 1 kg pulse consumption scenario, the climate impact of green and blue hydrogen decays

232 rapidly to zero within the first few decades (conversion of decayed CH<sub>4</sub> to CO<sub>2</sub> not included),  
233 whereas the climate impact of avoided CO<sub>2</sub> emissions becomes roughly stable with time.  
234 Continuous consumptions of hydrogen would lead to stable radiative forcing and temperature  
235 change at longer timescales with magnitudes depending on emission rates, and such impacts will  
236 adjust quickly if future emission rates change. Meanwhile, continuous consumption of fossil  
237 fuels leads to accumulation of CO<sub>2</sub> concentration and increasing climate responses. Even if CO<sub>2</sub>  
238 emission is ceased, its impacts would last for hundreds of years.

239 Under the high leakage scenario, the additional leakage of hydrogen (i.e., 10% vs. 1% hydrogen  
240 leakage rate) reduce the short-term climate benefits of green hydrogen, and the additional  
241 leakage of methane (i.e., 3% vs. 1% methane leakage rate) further lead to net disbenefits for blue  
242 hydrogen in the first few years, when compared to avoided CO<sub>2</sub> emissions (Fig. 2 and 3). In both  
243 the low and high leakage cases, methane adds more warming than does hydrogen (Fig. S5).  
244 Because of the shorter lifetimes of hydrogen and methane, net climate benefits for blue hydrogen  
245 are observed after ~ 12 and 20 years under different emission scenarios for the high leakage case.  
246 The climate impacts of hydrogen become orders of magnitude smaller than that of CO<sub>2</sub>  
247 emissions as time evolves.

248 In our central cases, we do not include methane leakages when calculating climate impacts for  
249 the avoided CO<sub>2</sub> emissions, but methane leakages are included for blue hydrogen. Under all  
250 emission scenarios, using the same methane leakage rates for methane combustion and hydrogen  
251 production (Fig. S6 and S7) substantially increases the warming potentials from the avoided CO<sub>2</sub>  
252 emissions, especially for the short-term responses, leading to net climate benefits for both clean  
253 hydrogen alternatives. Consideration of conversion of the decayed methane to CO<sub>2</sub> further  
254 increases the long-term climate impacts for both blue hydrogen and the avoided CO<sub>2</sub> emissions  
255 cases that contain methane leakage (Fig. S6 and S7). As in Ocko and Hamburg (2022),  
256 considering different amounts of avoided CO<sub>2</sub> emission for per kg hydrogen consumption (e.g., 5  
257 or 15 kg CO<sub>2</sub> avoided per kg hydrogen consumption) can affect both short-term and long-term  
258 climate impacts (Fig. S8). In contrast, considering different hydrogen perturbation lifetimes or  
259 climate response functions has minor effects (Fig. S6, S7, and S9). Here we do not cover all  
260 uncertainties, but give some first-level impressions of how different parameters can affect results  
261 presented in this analysis.

262 Finally, Ocko and Hamburg (2022) quantified the net climate benefits of consuming hydrogen  
263 compared to the avoided CO<sub>2</sub> emissions by comparing the time-integrated radiative forcing from  
264 continuous emissions of both gases. This metric over-predicts the amount of warming that would  
265 be produced by methane and hydrogen leakage relative to the warming that would have been  
266 caused by the avoided CO<sub>2</sub> emissions over time (Fig. S10). This result is similar to that of (Allen  
267 et al., 2016) showing that, for pulse emissions and any time horizon longer than a decade, the  
268 global mean relative temperature response metric (i.e., GTP) would be lower than values of the  
269 time-integrated relative radiative forcing (i.e., GWP).

## 270 **Discussion**

271 The radiative forcing calculation presented here is a linear approximation, with radiative forcing  
272 increasing linearly with concentration, when in fact absorption bands become increasingly  
273 saturated at higher concentrations, and this results in less sensitivity at higher concentrations.  
274 The radiative forcing calculation assumes an unchanging background atmospheric composition,  
275 whereas it is likely that the climate impact of an emission will depend on the background climate  
276 state (Duan et al., 2019; Robrecht et al., 2019). For instance, the indirect radiative forcing of  
277 hydrogen through its effect on methane's lifetime might depend on the background methane  
278 concentration. The effectiveness of radiative forcing at affecting temperature can vary  
279 substantially from gas to gas (Hansen et al., 1997; Modak et al., 2018). In addition, the  
280 framework used here only compares hydrogen with the avoided CO<sub>2</sub> emissions, while fossil fuel  
281 adaptation are associated with emissions of other radiatively active species and air pollutants (on  
282 Climate Change, 2018).

283 Many important uncertainties persist. For example, we considered the chemical adjustments to  
284 radiative forcing for methane due to effects on ozone and stratospheric water vapor, as  
285 considered by Ocko and Hamburg (2022). There are other effects that have been included in  
286 previous works, which would affect the warming impact of methane emissions (Boucher et al.,  
287 2009; Shindell et al., 2009). There are uncertainties related to cloud radiative effects from  
288 thermodynamic adjustments and aerosol-cloud interactions (O'Connor et al., 2022). There are  
289 additional uncertainties related to the fast physical radiative forcing adjustments to dioxide,  
290 ozone and other radiatively active gases (Smith et al., 2018). Co-emissions from fossil fuel  
291 combustions (e.g., aerosol precursors) can also affect climate and public health (Lelieveld et al.,

292 2019). Unlike the long-lived CO<sub>2</sub>, the climate impact of short-lived forcers might depend on  
293 locations of emissions (Persad and Caldeira, 2018; Burney et al., 2022). While their radiative  
294 forcing might diminish quickly after emission ceasing, indirect impacts from these short-lived  
295 forcers (e.g., by affecting carbon sinks and atmospheric CO<sub>2</sub> levels) could last longer,  
296 introducing additional uncertainties (Fu et al., 2020). None of these considerations are expected  
297 to be of sufficient magnitudes to qualitatively alter key conclusions presented here.

298 Ocko and Hamburg (2022) proposes a metric, which we call CAGWP, that involves the integral  
299 of radiative forcing for a sustained emission, which differs from the standard GWP metric based  
300 on a unit emission of 1 kg of gas. While the Global Warming Potential metric (GWP) has been  
301 widely used to compare the climate impact of different greenhouse gases, it may not be the best  
302 predictor of climate impacts. For example, Allen et al. (2016) have argued that the GWP metric  
303 over-emphasizes the long-term climate effect of short-lived gases such as methane. The CAGWP  
304 metric proposed by Ocko and Hamburg (2022) emphasizes short-lived gases to an even greater  
305 extent than the customary GWP metrics. We have shown that the CAGWP metric is equivalent  
306 to a front-loaded weighted integral of a pulse emission. The 100-year CAGWP metric weights  
307 the first year after an emission 99 times, whereas it weights the 99<sup>th</sup> year after an emission only  
308 once.

309 There are different motivations for reducing warming at various timescales. One motivation is to  
310 avoid near-term climate damage that might come, for example, from increasing storm or drought  
311 intensity. Another motivation is to avoid long-term climate damage that might come, for  
312 example, from the melting of the large ice sheets (Pattyn et al., 2018) or making parts of the  
313 tropics effectively uninhabitable (Dunne et al., 2013; Sun et al., 2019). Decision-making can  
314 balance near-term and long-term risks, and look for opportunities to address both kinds of risk  
315 simultaneously.

316 Different climate forcing agents differ in their degree of reversibility. To a close approximation,  
317 on the time scale of decades or more, temperature change from methane or hydrogen emissions  
318 are proportional to rates of emission whereas temperature change from carbon dioxide is  
319 proportional to cumulative emission (Jones et al., 2006; Allen et al., 2009). This important  
320 distinction is not captured by the CAGWP metric proposed by Ocko and Hamburg (2022).

321 Considering how different market sizes would affect the overall impact of hydrogen is beyond  
322 the scope of this analysis. Blue hydrogen, despite its larger climate impacts, is currently the  
323 dominate way of producing hydrogen. Meanwhile, the additional climate benefits from green  
324 hydrogen have been recognized that will likely play a greater role in some regions (EUR-Lex,  
325 2022) in the future. It is clear that electrolytic hydrogen made with carbon-emission-free  
326 electricity would produce less climate change than hydrogen made using methane as a feedstock;  
327 people use steam-methane reforming of methane to produce hydrogen typically because it costs  
328 less than electrolysis.

### 329 **Conclusion**

330 Our analysis confirms the results of Ocko and Hamburg (2022) under consistent assumptions but  
331 complements their presentation with additional uncertainty analysis and a longer-term  
332 perspective. While we confirm the results presented in Ocko and Hamburg (2022), it is clear that  
333 over longer time horizons (e.g., 100 years) substituting blue or green hydrogen for fossil fuels  
334 will result in much less climate change.

335 We have developed a tutorial for the derivations of underlying differential equations that  
336 describe radiative forcing of hydrogen emissions, which differ slightly from equations relied on  
337 by previous studies. In line with previous studies (Fuglestvedt et al., 2010; Allen et al., 2016;  
338 Balcombe et al., 2018), both the radiative forcing and global mean temperature response from  
339 hydrogen and methane are proportional to the underlying emission rates, whereas climate  
340 impacts from carbon dioxide are closely related to cumulative emissions. For the same quantity  
341 of emissions, hydrogen shows consistently smaller climate impact than methane. High emission  
342 rates of methane contribute primarily to the high warming potential of methane-derived  
343 hydrogen production, with high hydrogen leakage rates playing a secondary role. As shown by  
344 Ocko and Hamburg (2022), blue hydrogen with a methane leakage rate of 3% and a hydrogen  
345 leakage rate of 10% could produce more warming in the first 20 years after the release. However,  
346 even with these high leakage rates, warming from blue hydrogen 100 years later would be only a  
347 small portion of the warming from the fossil fuels it replaced. In contrast to the climate impact of  
348 carbon dioxide emissions, which persist for many millennia (Archer, 2005; Solomon et al.,  
349 2009), climate impacts decay on the timescale of decades after a cessation of methane or  
350 hydrogen emissions.

351 Consideration of methane leakage associated with burning natural gas can have a substantial  
352 effect on results. Including the methane leakage associated with fossil fuel combustion would  
353 increase its short-term impact and might lead to net short-term climate benefit for blue hydrogen.  
354 Other factors, including the hydrogen lifetime and different climate response functions, are  
355 relatively less important.

356 Ocko and Hamburg (2022) proposes that the climate impact of blue and green hydrogen be  
357 evaluated with the use of a metric that strongly weights near-term radiative forcing relative to  
358 long-term radiative forcing from individual pulse emissions.

359 We emphasize that to attain near-term climate benefits from “blue” hydrogen that dominates  
360 current market depends critically on achieving low methane leakage rates. “Green” hydrogen  
361 produced by electrolysis using carbon-emission-free electricity has a small climate impact  
362 relative to the impact of the fossil fuels that hydrogen would replace, while very high hydrogen  
363 leakage rates could pose some climate concern and undercut accomplishing net zero emission  
364 goals. Safety and cost considerations may motivate reduction of hydrogen leakage (Nugroho et  
365 al., 2022), In all cases considered, relative to fossil fuel combustion and associated emissions,  
366 both “blue” and “green” hydrogen show large long-term climate benefits even with high leakage  
367 rates.

### 368 **Code availability**

369 Scripts used to derive equations presented in this analysis are written in Wolfram Mathematica  
370 and are available online at <https://doi.org/10.5281/zenodo.7346379>. Scripts used to calculate  
371 numbers and plot figures in this analysis are written in Python and are available online at  
372 <https://doi.org/10.5281/zenodo.7346379>.

### 373 **Author contribution**

374 Lei Duan and Ken Caldeira designed the simulations, developed the equations, and did the  
375 calculations. Lei Duan prepared the initial manuscript and both of them reviewed and edited the  
376 manuscript.

### 377 **Competing interests**

378 The authors declare that they have no conflict of interest. However, in the interest of  
379 transparency, we would like to point out that K.C. is an employee of a non-profit organization



380 that funds early commercial demonstration projects related to clean alternatives that can displace  
381 carbon-intensive technologies, and this can include clean hydrogen to decarbonize industry. In  
382 the further interest of transparency, note that L.D. is a consultant for a for-profit entity that has  
383 no known investments related to clean hydrogen.

384 **Acknowledgements**

385 This work is supported by a gift from Gates Ventures LLC to the Carnegie Institution for  
386 Science. The authors thank Leslie Willoughby for language polishing.

387 **Reference**

- 388 Allen, M. R., Frame, D. J., Huntingford, C., Jones, C. D., Lowe, J. A., Meinshausen, M., and  
389 Meinshausen, N.: Warming caused by cumulative carbon emissions towards the trillionth tonne,  
390 *Nature*, 458, 1163–1166, 2009.
- 391 Allen, M. R., Fuglestvedt, J. S., Shine, K. P., Reisinger, A., Pierrehumbert, R. T., and Forster, P.  
392 M.: New use of global warming potentials to compare cumulative and short-lived climate  
393 pollutants, *Nat. Clim. Chang.*, 6, 773–776, 2016.
- 394 EUR-Lex: <https://eur-lex.europa.eu/legal-content/EN/TXT/?uri=CELEX:52020DC0301>, last  
395 access: 23 November 2022.
- 396 Archer, D.: Fate of fossil fuel CO<sub>2</sub> in geologic time, *J. Geophys. Res. C: Oceans*, 2005.
- 397 Balcombe, P., Speirs, J. F., Brandon, N. P., and Hawkes, A. D.: Methane emissions: choosing the  
398 right climate metric and time horizon, *Environ. Sci. Process. Impacts*, 20, 1323–1339, 2018.
- 399 Boucher, O., Friedlingstein, P., Collins, B., and Shine, K. P.: The indirect global warming  
400 potential and global temperature change potential due to methane oxidation, *Environ. Res. Lett.*,  
401 4, 044007, 2009.
- 402 Burney, J., Persad, G., Proctor, J., Bendavid, E., Burke, M., and Heft-Neal, S.: Geographically  
403 resolved social cost of anthropogenic emissions accounting for both direct and climate-mediated  
404 effects, *Science Advances*, 8, eabn7307, 2022.
- 405 on Climate Change, I. P.: Global warming of 1.5° C: An IPCC special report on the impacts of  
406 global warming of 1.5° C above pre-industrial levels and related global greenhouse gas emission  
407 pathways, in the context of strengthening the global response to the threat of climate change,  
408 sustainable development, and efforts to eradicate poverty, Intergovernmental Panel on Climate  
409 Change, 2018.
- 410 Duan, L., Cao, L., and Caldeira, K.: Estimating contributions of sea ice and land snow to climate  
411 feedback, *J. Geophys. Res.*, 124, 199–208, 2019.
- 412 Dunne, J. P., Stouffer, R. J., and John, J. G.: Reductions in labour capacity from heat stress under  
413 climate warming, *Nat. Clim. Chang.*, 3, 563–566, 2013.
- 414 Forster, P., Storelvmo, T., Armour, K., Collins, W., Dufresne, J.-L., Frame, D., Lunt, D.,  
415 Mauritsen, T., Palmer, M., Watanabe, M., Wild, M., and Zhang, H.: The Earth’s Energy Budget,  
416 Climate Feedbacks, and Climate Sensitivity, in: *Climate Change 2021: The Physical Science  
417 Basis. Contribution of Working Group I to the Sixth Assessment Report of the  
418 Intergovernmental Panel on Climate Change*, edited by: Masson-Delmotte, V., P. Zhai, A. Pirani,  
419 S.L. Connors, C. Péan, S. Berger, N. Caud, Y. Chen, L. Goldfarb, M.I. Gomis, M. Huang, K.  
420 Leitzell, E. Lonnoy, J.B.R. Matthews, T.K. Maycock, T. Waterfield, O. Yelekçi, R. Yu, and B.  
421 Zhou, Cambridge University Press, Cambridge, United Kingdom and New York, NY, USA,  
422 923–1054, 2021.

423 Fu, B., Gasser, T., Li, B., Tao, S., Ciais, P., Piao, S., Balkanski, Y., Li, W., Yin, T., Han, L., Li,  
424 X., Han, Y., An, J., Peng, S., and Xu, J.: Short-lived climate forcers have long-term climate  
425 impacts via the carbon–climate feedback, *Nat. Clim. Chang.*, 10, 851–855, 2020.

426 Fuglestedt, J. S., Shine, K. P., Berntsen, T., Cook, J., Lee, D. S., Stenke, A., Skeie, R. B.,  
427 Velders, G. J. M., and Waitz, I. A.: Transport impacts on atmosphere and climate: Metrics,  
428 *Atmos. Environ.* (1994), 44, 4648–4677, 2010.

429 Gasser, T., Peters, G. P., Fuglestedt, J. S., Collins, W. J., Shindell, D. T., and Ciais, P.:  
430 Accounting for the climate–carbon feedback in emission metrics, *Earth Syst. Dyn.*, 8, 235–253,  
431 2017.

432 Geoffroy, O., Saint-Martin, D., Olivié, D. J. L., Voldoire, A., Bellon, G., and Tytéca, S.:  
433 Transient Climate Response in a Two-Layer Energy-Balance Model. Part I: Analytical Solution  
434 and Parameter Calibration Using CMIP5 AOGCM Experiments, *J. Clim.*, 26, 1841–1857, 2013.

435 Hansen, J., Sato, M., and Ruedy, R.: Radiative forcing and climate response, *J. Geophys. Res.*,  
436 102, 6831–6864, 1997.

437 Jones, C. D., Cox, P. M., and Huntingford, C.: Climate-carbon cycle feedbacks under  
438 stabilization: uncertainty and observational constraints, *Tellus B Chem. Phys. Meteorol.*, 58,  
439 603–613, 2006.

440 Lelieveld, J., Klingmüller, K., Pozzer, A., Burnett, R. T., Haines, A., and Ramanathan, V.:  
441 Effects of fossil fuel and total anthropogenic emission removal on public health and climate,  
442 *Proc. Natl. Acad. Sci. U. S. A.*, 116, 7192–7197, 2019.

443 Modak, A., Bala, G., Caldeira, K., and Cao, L.: Does shortwave absorption by methane influence  
444 its effectiveness?, *Clim. Dyn.*, 51, 3653–3672, 2018.

445 Myhre, G., Shindell, D., Bréon, F.-M., Collins, W., Fuglestedt, J., Huang, J., Koch, D.,  
446 Lamarque, J.-F., Lee, D., Mendoza, B., Nakajima, T., Robock, A., Stephens, G., Takemura, T.,  
447 and Zhang, H.: Anthropogenic and Natural Radiative Forcing, in: *Climate change 2013 : the*  
448 *physical science basis; Working Group I contribution to the fifth assessment report of the*  
449 *Intergovernmental Panel on Climate Change*, edited by: Stocker, T.F., Qin, G.-K., Plattner, M.,  
450 Tignor, S.K., Allen, J., Boschung, A., Nauels, Y., Xia, V. Bex and P.M. Midgley, Cambridge  
451 University Press, Cambridge, United Kingdom and New York, NY, USA., 659–740, 2013.

452 Nugroho, F. A. A., Bai, P., Darmadi, I., Castellanos, G. W., Fritzsche, J., Langhammer, C.,  
453 Rivas, J. G., and Baldi, A.: Inverse Designed Plasmonic Metasurface with ppb Optical Hydrogen  
454 Detection, *ChemRxiv*, <https://doi.org/10.26434/chemrxiv-2022-9vhsn>, 2022.

455 Ocko, I. B. and Hamburg, S. P.: Climate consequences of hydrogen emissions, *Atmos. Chem.*  
456 *Phys.*, 22, 9349–9368, 2022.

457 O’ Connor, F. M., Johnson, B. T., Jamil, O., Andrews, T., Mulcahy, J. P., and Manners, J.:  
458 Apportionment of the pre-industrial to present-day climate forcing by methane using UKESM1:

459 The role of the cloud radiative effect, *J. Adv. Model. Earth Syst.*, 14,  
460 <https://doi.org/10.1029/2022ms002991>, 2022.

461 Pattyn, F., Ritz, C., Hanna, E., Asay-Davis, X., DeConto, R., Durand, G., Favier, L., Fettweis,  
462 X., Goelzer, H., Golledge, N. R., Kuipers Munneke, P., Lenaerts, J. T. M., Nowicki, S., Payne,  
463 A. J., Robinson, A., Seroussi, H., Trusel, L. D., and van den Broeke, M.: The Greenland and  
464 Antarctic ice sheets under 1.5 °C global warming, *Nat. Clim. Chang.*, 8, 1053–1061, 2018.

465 Persad, G. G. and Caldeira, K.: Divergent global-scale temperature effects from identical  
466 aerosols emitted in different regions, *Nat. Commun.*, 9, 3289, 2018.

467 Robrecht, S., Vogel, B., Grooß, J.-U., Rosenlof, K., Thornberry, T., Rollins, A., Krämer, M.,  
468 Christensen, L., and Müller, R.: Mechanism of ozone loss under enhanced water vapour  
469 conditions in the mid-latitude lower stratosphere in summer, *Atmos. Chem. Phys.*, 19, 5805–  
470 5833, 2019.

471 Shindell, D. T., Faluvegi, G., Koch, D. M., Schmidt, G. A., Unger, N., and Bauer, S. E.:  
472 Improved attribution of climate forcing to emissions, *Science*, 326, 716–718, 2009.

473 Smith, C. J., Kramer, R. J., Myhre, G., Forster, P. M., Soden, B. J., Andrews, T., Boucher, O.,  
474 Faluvegi, G., Fläschner, D., Hodnebrog, Ø., Kassoar, M., Kharin, V., Kirkevåg, A., Lamarque, J.-  
475 F., Mülmenstädt, J., Olivié, D., Richardson, T., Samset, B. H., Shindell, D., Stier, P., Takemura,  
476 T., Voulgarakis, A., and Watson-Parris, D.: Understanding Rapid Adjustments to Diverse  
477 Forcing Agents, *Geophys. Res. Lett.*, 45, 12023–12031, 2018.

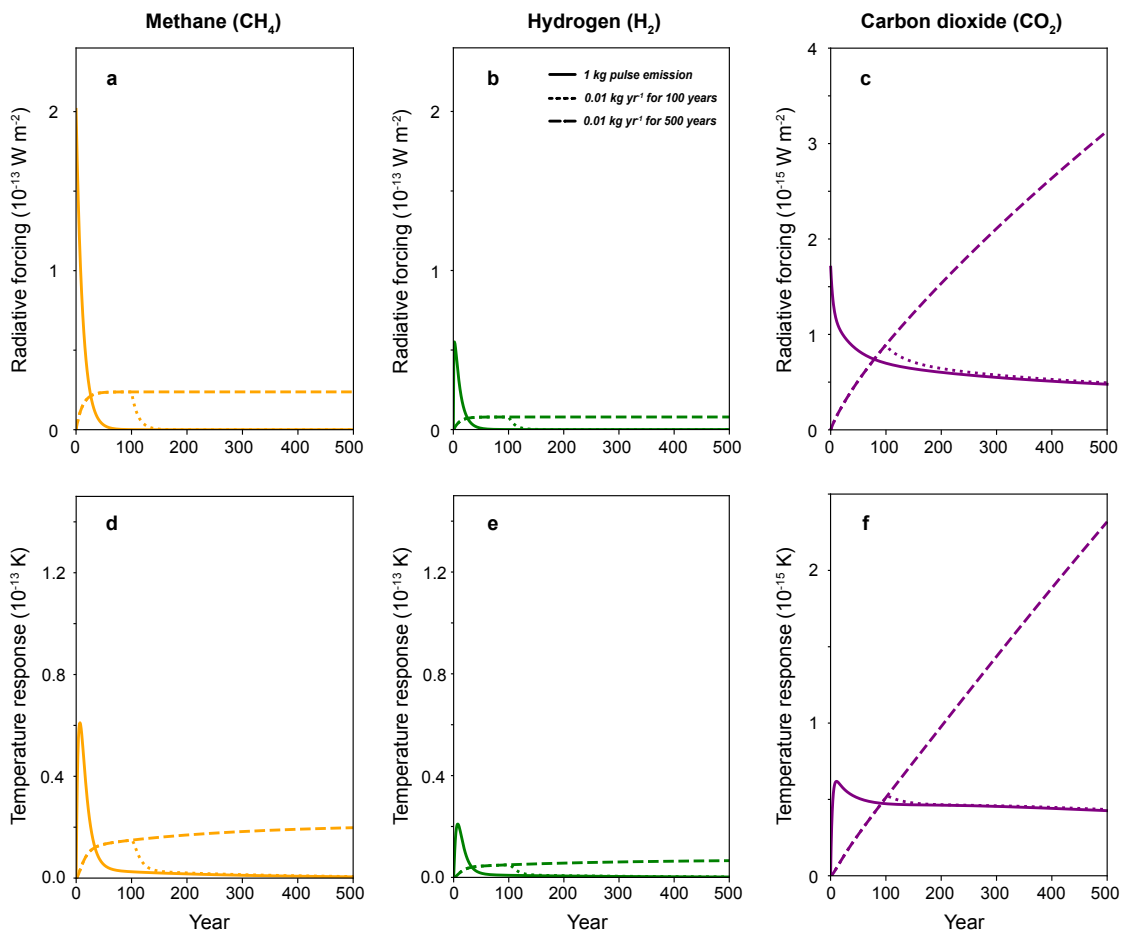
478 Solomon, S., Plattner, G.-K., Knutti, R., and Friedlingstein, P.: Irreversible climate change due to  
479 carbon dioxide emissions, *Proc. Natl. Acad. Sci. U. S. A.*, 106, 1704–1709, 2009.

480 Sun, Q., Miao, C., Hanel, M., Borthwick, A. G. L., Duan, Q., Ji, D., and Li, H.: Global heat  
481 stress on health, wildfires, and agricultural crops under different levels of climate warming,  
482 *Environ. Int.*, 128, 125–136, 2019.

483 Warwick, N., Griffiths, P., Keeble, J., Archibald, A., and Pyle, J.: Atmospheric implications of  
484 increased Hydrogen use, [https://www.gov.uk/government/publications/atmospheric-](https://www.gov.uk/government/publications/atmospheric-implications-of-increased-hydrogen-use)  
485 [implications-of-increased-hydrogen-use](https://www.gov.uk/government/publications/atmospheric-implications-of-increased-hydrogen-use), 8 April 2022.

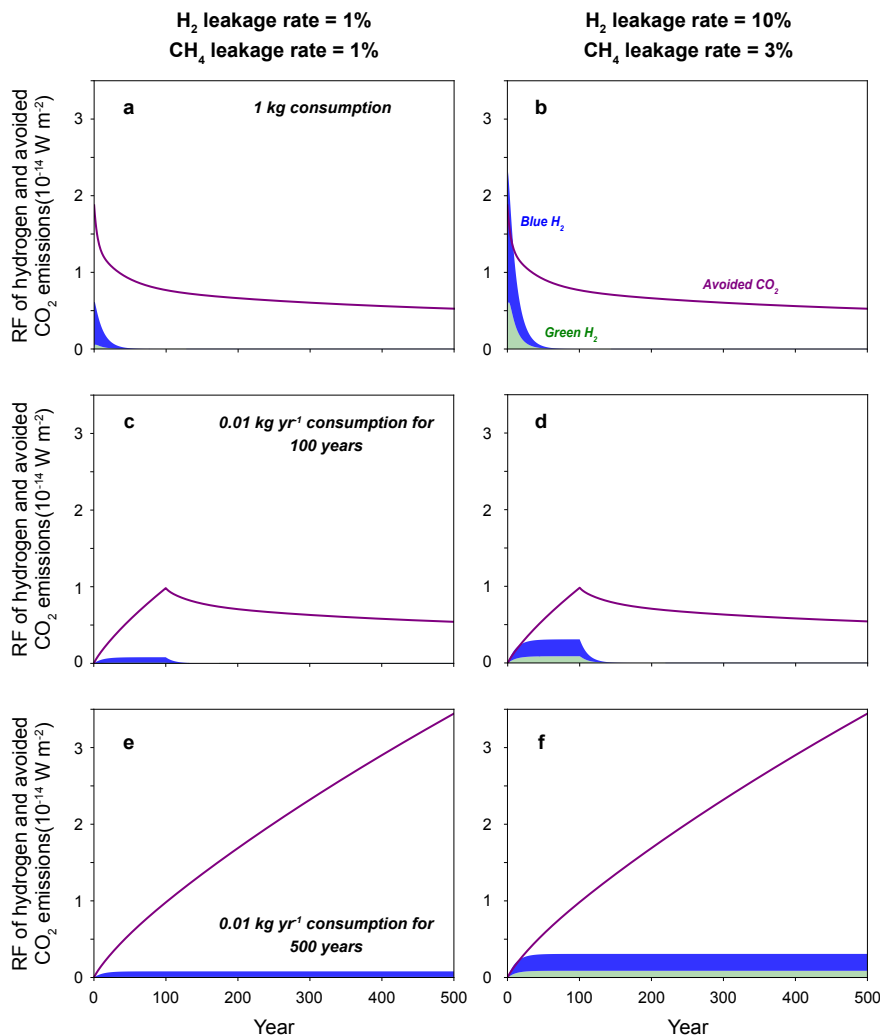
486

487 **Figure 1.** Climate impact from emissions of different species. **(a-c)** Radiative forcing and **(d-f)**  
 488 global mean temperature response caused by emissions of methane (CH<sub>4</sub>), hydrogen (H<sub>2</sub>), and  
 489 carbon dioxide (CO<sub>2</sub>). Three emission scenarios are considered: a 1 kg pulse emission, a 0.01 kg  
 490 yr<sup>-1</sup> continuous emission lasting for 100 years, and a 0.01 kg yr<sup>-1</sup> continuous emission lasting for  
 491 500 years. CH<sub>4</sub> and H<sub>2</sub> share the same y-axis, the maximum value of which is 60 times relative to  
 492 that of CO<sub>2</sub>. Radiative forcing from a continuous emission of hydrogen and methane is  
 493 proportional to emission rates, and decays rapidly once ceased, whereas radiative forcing from  
 494 carbon dioxide is closely related to cumulative emissions and will last for longer timescales.  
 495 Figures showing only 100-year results are plotted in Figure S12.



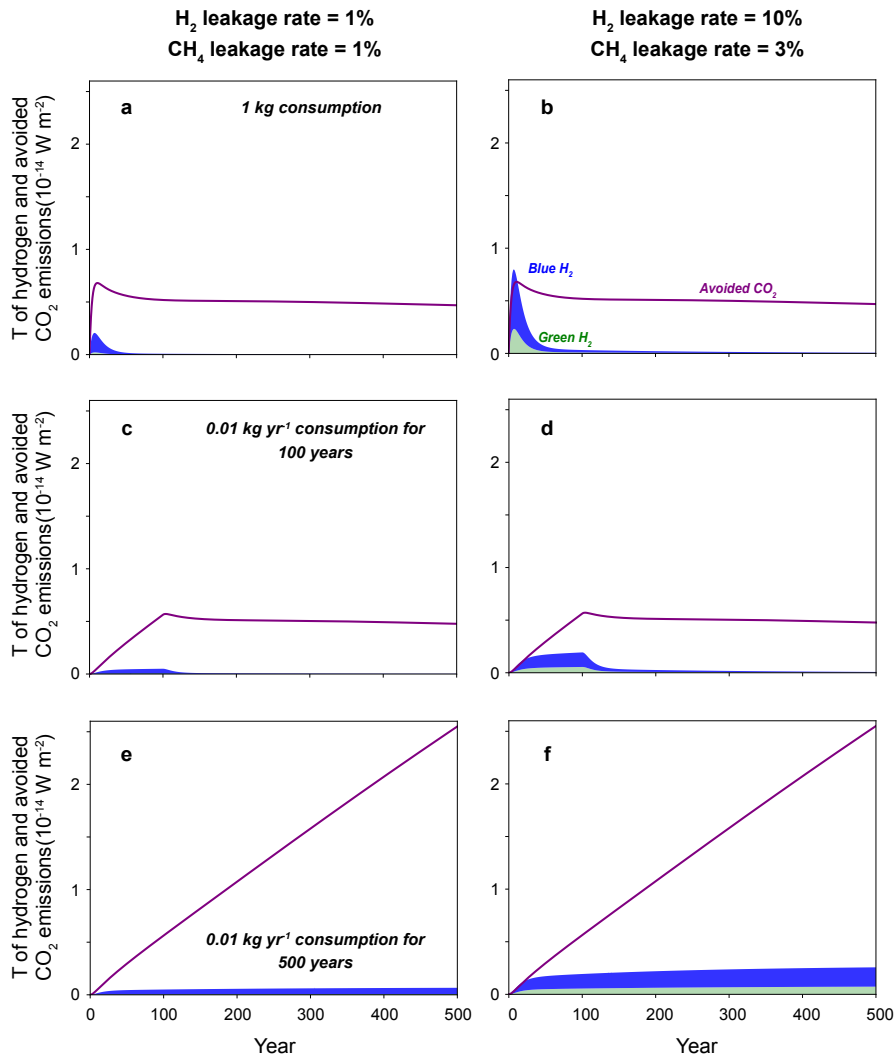
496

497 **Figure 2.** Radiative forcing from consumptions of green hydrogen, blue hydrogen, and avoided  
 498 CO<sub>2</sub> emissions. Three cases are considered: (a-b) a 1 kg consumption of hydrogen, (c-d) a 0.01  
 499 kg yr<sup>-1</sup> continuous consumption of hydrogen lasting for 100 years, and (e-f) a 0.01 kg yr<sup>-1</sup>  
 500 continuous consumption of hydrogen lasting for 500 years. The left column shows cases with 1%  
 501 hydrogen and 1% methane leakage rates, and the right column shows cases with 10% hydrogen  
 502 and 3% methane leakage rates. Methane leakage contributes primarily to the warming potential  
 503 of blue hydrogen consumption, while hydrogen leakage plays a secondary role. For the longer-  
 504 term, radiative forcing from carbon dioxide is substantially larger than that from clean hydrogen  
 505 alternatives. Figures showing only 100-year results are plotted in Figure S13.



506

507 **Figure 3.** Same as Figure 2 but for the global mean temperature response. Figures showing only  
508 100-year results are plotted in Figure S14.



509